

Small-signal stability of power systems with voltage droop

Jakob Niehues, Robin Delabays, and Frank Hellmann

Abstract—The small-signal stability of power grids is a well-studied topic. In this work, we give new sufficient conditions for highly heterogeneous mixes of grid-forming inverters (and other machines) that implement a V - q droop to stabilize viable operating states of lossless grids. Assuming the edges are not overloaded, and static voltage limits are satisfied, our conditions are fully local: They can be evaluated bus by bus without information on the rest of the grid. Other than the presence of V - q droop, we make no model assumptions. In particular, we do not assume a specific control strategy of the inverters, the number, or type, of their internal degrees of freedom, or that the control is homogeneous throughout the system.

We achieve this by recasting the dynamics of the nodes as a complex frequency reaction to an active and reactive power signal coming from the grid. By working directly in terms of the node's linearized complex frequency response, the transfer functions capturing the linear response do not depend on arbitrary phases. Further, they are easily interpretable as the frequency/amplitude reaction to active/reactive power imbalance, and correspond directly to the typical design considerations for grid-forming control. By exploiting the presence of the V - q droop, we can ensure that the grid's active/reactive power response to a frequency/amplitude change is semi-sectorial. This allows us to use an adapted small phase theorem to obtain local sufficient stability conditions for edges and nodes, which also yields novel results for established control designs.

Index Terms—grid-forming control, droop control, complex frequency, voltage source converter, small-signal stability

I. INTRODUCTION

The analysis of the small-signal stability of multi-machine power grids is one of the central topics of power grid analysis. The main result of the seminal paper of [1] was to give conditions under which multiple machines and loads, modeled as oscillators, are stable to small perturbations.

Corresponding author: jakob.niehues@pik-potsdam.de
Potsdam Institute for Climate Impact Research (PIK), Member of the Leibniz Association, P.O. Box 60 12 03, D-14412 Potsdam, Germany (J.N., F.H.)

Technische Universität Berlin, ER 3-2, Hardenbergstrasse 36a, 10623 Berlin, Germany (J.N.)

School of Engineering, University of Applied Sciences of Western Switzerland HES-SO, Sion, Switzerland (R.D.)

Since then, a plethora of results from power engineering [2], control theory [3], [4] and theoretical physics [5] have expanded our understanding of the small signal stability of power systems.

The question has gained renewed interest with the advent of grid-forming converters. These converters are expected to provide the backbone to stabilize the synchronous operation of highly renewable future power grids [6]. Yet, detailed machine models are not known, and grid-forming control remains an active topic of research [7]. There is a wide range of stability results for concrete control strategies, as reviewed in [8]. However, most of them are *ad hoc* and do not generalize naturally to other control schemes.

In this paper we give a fully decentralized stability condition based on the transfer functions that capture how a grid-forming node's frequency and relative voltage velocity react to deviations from power, reactive power and voltage set points. Remarkably, our results are technology-neutral and apply to all nodal actors for which the response to reactive power and voltage set point deviations is proportional, which is an established principle, see for example [9], [10].

These variables correspond to working with the complex frequency [11] and describing the network state using time invariant variables that nevertheless fully characterize the operating state at the desired frequency [12], [13]. Such variables have been shown to be highly effective for identifying grid-forming behavior in the grid [14]. A key advantage of working in these quantities is that the transfer operators do not depend on arbitrary quantities such as phase angles. The resulting stability conditions are more explicit, simpler and more easily interpreted than, for example, those of [15], [16]. In particular, the transfer operators often do not explicitly depend on the operation point around which we linearize, and the conditions can be mapped back to system parameters immediately. We demonstrate this by recovering several classic results as special cases.

As in [15], [16], the central ingredient to our result is the small phase theory of [17]. A companion paper to this work [?] explores the application of this approach to adaptive networks, and demonstrates that these methods can match necessary conditions in that setting.

II. STATEMENT OF THE MAIN RESULT

For the sake of clarity, we begin with giving the main result, using the bare minimum of notation and concepts required to state it.

Consider a power grid model with negligible losses, admittance matrix \mathbf{Y} , and nodal complex voltages \mathbf{v} ,

$$v_n = V_n e^{j\varphi_n} = e^{\theta_n}, \quad (1)$$

thus $\varphi_n = \Im(\theta_n)$. The nodal current injections are $\mathbf{i} = \mathbf{Y}\mathbf{v}$, and the nodal power injections $p_n + jq_n = v_n \bar{i}_n$.

Denote the quantities at operating point with a superscript $^\circ$. In the co-rotating frame with the grid's nominal frequency, the operating point is given by constant v_n° that induce V_n° , φ_n° , and a power flow solution p_n° , q_n° matching the set point.

The derivative of the complex phase $\theta_n = \ln v_n$ is the complex frequency $\eta_n = \dot{\theta}_n = \varrho_n + j\omega_n$ (see [11], [12] for details). Its real part $\varrho_n = \frac{\dot{V}_n}{V_n}$ is the relative amplitude velocity, and its imaginary part, $\omega_n = \dot{\varphi}_n$, is the angular velocity, which is proportional to the frequency. Without loss of generality, we take the complex frequency at the operational state to be equal to zero: $\omega^\circ = \varrho^\circ = 0$.

We can understand the behavior of a broad class of dynamical actors in power grids by considering how their complex frequency changes in response to changes in the network state. Near the power flow solution of interest, we can consider the linearized response in terms of the transfer functions. Since grid-forming actors take the current as input and supply a voltage as output, we can choose p_n and q_n to represent the state of the system as seen from the node n . We restrict our analysis to actors that react to a deviation in q_n in the same way that they react to an internal deviation in V_n . This means the nodal response can be written in terms of some variable $\hat{q}_n := q_n + \alpha_n V_n$ that implements a droop-like relationship between q_n and V_n with proportionality coefficient $\alpha_n \in \mathbb{R}$. We then have four transfer functions $T_n^{\bullet\bullet}(s) \in \mathbb{C}$ that describe the nodal behavior near the power flow of interest:

$$\begin{bmatrix} \varrho_n \\ \omega_n \end{bmatrix} = - \begin{bmatrix} T_n^{\varrho\hat{q}} & T_n^{\varrho p} \\ T_n^{\omega\hat{q}} & T_n^{\omega p} \end{bmatrix} \begin{bmatrix} \Delta\hat{q}_n \\ \Delta p_n \end{bmatrix} =: -\mathbf{T}_n \begin{bmatrix} \Delta\hat{q}_n \\ \Delta p_n \end{bmatrix}, \quad (2)$$

where all quantities except α_n depend on the Laplace frequency s .

In Section V-B we show the kind of differential equations that lead to this type of transfer operators for the nodes. These are natural for a broad class of grid-forming actors. Following [12], the matrix elements of $\mathbf{T}_n(s)$ are expected to only depend on p° , q° and V° , but not on

the complex voltage v_n° directly. This is a key advantage of working in terms of quantities like p , q and η rather than, say, \dot{v} , \bar{v} , and i , \bar{i} directly. Our main result is:

Theorem 1 (Small-signal stability of power grids with V - q droop). *Consider a lossless power grid with admittance Laplacian \mathbf{Y} and an operating point with voltage phase angles φ_n° and magnitudes V_n° . Denote the maximum voltage ratio γ_{\max} and maximum phase difference $\Delta\varphi_{\max}$ such that $\gamma_{\max}^{-1} < V_n^\circ/V_m^\circ < \gamma_{\max}$ and $|\varphi_n^\circ - \varphi_m^\circ| < \Delta\varphi_{\max} < \pi/2$ for all n and m connected by a line.*

If the small-signal response of all nodes can be described by $\mathbf{T}_n(s)$ and α_n as in (2), and they satisfy

$$\Re(T_n^{\varrho\hat{q}}) + \Re(T_n^{\omega p}) > 0, \quad (3)$$

$$\Re(T_n^{\varrho\hat{q}}) \cdot \Re(T_n^{\omega p}) > \frac{1}{4} \left| T_n^{\varrho p} + \bar{T}_n^{\omega\hat{q}} \right|^2, \quad (4)$$

$$\alpha_n \geq 2V_n^\circ |Y_{nn}| \left(\frac{\gamma_{\max}}{\cos \Delta\varphi_{\max}} - 1 \right). \quad (5)$$

Then, the operating point is linearly stable.

Proof. We provide the proof in section VI. \square

These conditions align well with established practice in the design of grid-forming power grid actors. The diagonal terms $T_n^{\varrho\hat{q}}$ and $T_n^{\omega p}$ implement a stabilizing reaction of phase and amplitude to active and reactive power deviations, respectively. Equations (3)-(4) together imply that these transfer functions need to have negative real parts, i.e., they are stable. In addition, (4) quantifies how large the crosstalks $T_n^{\omega\hat{q}}$ between reactive power and frequency, and $T_n^{\varrho p}$ between active power and amplitude, may be, without endangering stability. From the physics of the interconnection, we get a third condition: that the stabilization of the amplitude is sufficiently strong relative to the coupling on the network, as quantified in (5). This condition relates the nodal V - q droop ratio α_n to the coupling via \mathbf{Y} , aggregated at node n , and global operational bounds. These bounds can also be given in decentralized form, see Section VI.

The remainder of this paper is structured as follows. In Section III and IV, we introduce notation and prove a new version of the Small Phase Theorem [17], that enables us to get decentralized stability conditions for networked systems. In VI we use this theorem to prove our main result. In Section VII, we interpret the main result along several examples from the literature. Finally, we outline generalizations in Section VIII.

III. NOTATION

To prove the above result, we begin by expanding on the notation used above. We want

to consider the small-signal stability of power grids with a heterogeneous mix of grid-forming actors. The N nodes are indexed n and m , $1 \leq n, m \leq N$. The E edges in the set of edges \mathcal{E} are indexed by ordered pairs $e = (n, m)$, $n < m$. For any nodal quantity x_n , we denote the overall N -dimensional vector by \mathbf{x} . We write $[\mathbf{x}]$ for the diagonal matrix with x_n on the diagonal: $[\mathbf{x}]_{nm} = \delta_{nm}x_n$. In general, matrices are uppercase bold, e.g., \mathbf{A} , and vectors are lower case bold. We denote with $\mathbf{1}$ the constant vector $1_n = 1$, so the identity matrix is $[\mathbf{1}] = \mathbf{I}$, and similarly for $\mathbf{0}$ and $[\mathbf{0}]$.

We denote the imaginary unit j , the complex conjugate of a quantity z by \bar{z} , the transpose of a vector or matrix \mathbf{A} as \mathbf{A}^\top and the complex transpose by \mathbf{A}^\dagger .

We will often have two quantities per node, e.g., z_n and \bar{z}_n . Stacking the vector of nodal quantities is written as

$$\begin{bmatrix} z \\ \bar{z} \end{bmatrix}, \quad (6)$$

We also will often be looking only at the components associated to a single node n in such a stacked vector. To this end, we introduce the matrix \mathbf{P}_n which selects these entries

$$\begin{bmatrix} z_n \\ \bar{z}_n \end{bmatrix} = \mathbf{P}_n \begin{bmatrix} z \\ \bar{z} \end{bmatrix}, \quad (7)$$

and its transpose \mathbf{P}_n^\dagger . Note that \mathbf{P}_n are isometries, and $\mathbf{P}_n^\dagger \mathbf{P}_n$ is an orthogonal projection operator.

Given a set of nodewise matrices \mathbf{A}_n , the matrix built from them with the direct sum \bigoplus then acts on our stacked vector as:

$$\bigoplus_n \mathbf{A}_n \begin{bmatrix} z \\ \bar{z} \end{bmatrix} := \sum_n \mathbf{P}_n^\dagger \mathbf{A}_n \mathbf{P}_n \begin{bmatrix} z \\ \bar{z} \end{bmatrix}, \quad (8)$$

While the matrix representation of $\bigoplus_n \mathbf{A}_n$ is not block diagonal on the stacking $[z \ \bar{z}]^\top$, it is block diagonal when stacking $[z_1 \ \bar{z}_1 \ z_2 \ \bar{z}_2 \ \dots \ z_n \ \bar{z}_n]^\top$.

We also introduce the matrix \mathbf{P}_e that selects the states related to the edge e from our stacked vector:

$$\mathbf{P}_e \begin{bmatrix} z \\ \bar{z} \end{bmatrix} = \mathbf{P}_{(n,m)} \begin{bmatrix} z \\ \bar{z} \end{bmatrix} = \begin{bmatrix} z_n \\ z_m \\ \bar{z}_n \\ \bar{z}_m \end{bmatrix}. \quad (9)$$

The \mathbf{P}_e are isometries, but $\mathbf{P}_e^\dagger \mathbf{P}_e$ are not mutually orthogonal. Therefore, an operator built from 4×4 matrices \mathbf{A}_e as

$$\sum_e \mathbf{P}_e^\dagger \mathbf{A}_e \mathbf{P}_e, \quad (10)$$

is not block diagonal. However, it can be written as the projection of a block diagonal operator $\bigoplus_e \mathbf{A}_e$ and we write:

$$\sum_e \mathbf{P}_e^\dagger \mathbf{A}_e \mathbf{P}_e = \mathbf{B}_+^\dagger \bigoplus_e \mathbf{A}_e \mathbf{B}_+. \quad (11)$$

IV. PHASE STABILITY PRELIMINARIES

Our results are based on the Generalized Small Phase Theorem of Chen *et al.* [17]. We prove a straightforward proposition stating that if the transfer operators of the system under consideration have a block structure, the global stability conditions can be decomposed into local conditions. An immediate application are networked systems that consist of node and edge variables that are coupled according to a graph.

Using this proposition we give a precise statement of the stability conditions for a power grid of general grid-forming grid actors with V - q droop as introduced above.

For completeness, we begin by recalling the Small Phase Theorem of [17], which provides conditions for the stability of the connected system $\mathbf{G}\#\mathbf{H}$, in terms of the *numerical range* W and the *angular field of values* W' [18, Sec. 1.0, Def. 1.1.2], [19], [20], defined for a matrix $\mathbf{M} \in \mathbb{C}^{N \times N}$ as

$$\begin{aligned} W(\mathbf{M}) &= \{z^\dagger \mathbf{M} z \mid z \in \mathbb{C}^N, z^\dagger z = 1\}, \\ W'(\mathbf{M}) &= \{z^\dagger \mathbf{M} z \mid z \in \mathbb{C}^N, z^\dagger z > 0\}. \end{aligned} \quad (12)$$

When the numerical range lies in a half complex plane, we introduce the notion of *sectoriality*. Assume that 0 is not in the interior of $W(\mathbf{M})$. Define $\bar{\phi}(\mathbf{M})$ and $\underline{\phi}(\mathbf{M})$ as the maximum and minimum arguments of the elements of such a $W(\mathbf{M})$, and $\delta(\mathbf{M}) := \bar{\phi}(\mathbf{M}) - \underline{\phi}(\mathbf{M})$. Then the matrix \mathbf{M} is

- *semi-sectorial* if $\delta(\mathbf{M}) \leq \pi$;
- *quasi-sectorial* if $\delta(\mathbf{M}) < \pi$;
- *sectorial* if $0 \notin W(\mathbf{M})$.

Notice that a non-sectorial matrix \mathbf{M} is semi-sectorial if 0 is on the boundary of $W(\mathbf{M})$.

Let $\mathcal{RH}_\infty^{m \times m}$ denote the set of $m \times m$ transfer matrices of real rational proper stable systems. For these systems, all the poles of any $\mathbf{H}(s) \in \mathcal{RH}_\infty^{m \times m}$ (should there be any) are in the open left-hand side of the plane. A system $\mathbf{G} \in \mathcal{RH}_\infty^{m \times m}$ is called frequency-wise sectorial if $\mathbf{G}(s)$ is sectorial for all $s \in j\mathbb{R}$. A system $\mathbf{G}(s)$ is semi-stable if its poles are in the closed left half plane. Take $j\Omega$ the set of poles on the imaginary axis, and $j\mathbb{R} \setminus j\Omega$ the indented imaginary axis with half-circles of radius $\epsilon \in \mathbb{R}$ around the poles and of radius $1/\epsilon$ around ∞ if it is a zero. We call this “the contour”. A system is semi-stable frequency-wise semi-sectorial if $\mathbf{G}(s)$ has constant rank and is semi-sectorial on $j\mathbb{R} \setminus j\Omega$.

The phase center is defined as $\gamma[\mathbf{G}(s)] := \{\bar{\phi}[\mathbf{G}(s)] + \underline{\phi}[\mathbf{G}(s)]\}/2$, and without loss of generality, we assume that $\gamma[\mathbf{G}(\epsilon^+)] := \lim_{\epsilon \searrow 0} \gamma[\mathbf{G}(\epsilon)] = 0$.

We can now recall Chen *et al.*'s Small Phase Theorem.

Theorem 2 (Generalized Small Phase Theorem, [17]). *Let \mathbf{G} be semi-stable frequency-wise semi-sectorial with $j\Omega$ being the set of poles on the imaginary axis, and $\mathbf{H} \in \mathcal{RH}_\infty$ be frequency-wise sectorial. Then $\mathbf{G}\#\mathbf{H}$ is stable if*

$$\sup_{s \in j[0, \infty] \setminus j\Omega} [\bar{\phi}(\mathbf{G}(s)) + \bar{\phi}(\mathbf{H}(s))] < \pi, \quad (14)$$

$$\inf_{s \in j[0, \infty] \setminus j\Omega} [\underline{\phi}(\mathbf{G}(s)) + \underline{\phi}(\mathbf{H}(s))] > -\pi. \quad (15)$$

Proof. See [17] \square

If the system $\mathbf{G}\#\mathbf{H}$ has a block structure, e.g., a networked distributed power system, we can show the following:

Proposition 3 (Generalized Small Phase Theorem with Block Structure). *Consider the system $\mathbf{G}\#\mathbf{H}$ with the block structure $\mathbf{H} = \bigoplus_n \mathbf{T}_n(s)$ and $\mathbf{G} = \mathbf{B}^\dagger \bigoplus_e \mathcal{T}_e(s) \mathbf{B}$ for some \mathbf{B} of appropriate dimensions. For each n , let $\mathbf{T}_n(s) \in \mathcal{RH}_\infty$ be frequency-wise sectorial. For each e , let $\mathcal{T}_e(s)$ be semi-stable frequency-wise semi-sectorial. Write $j\Omega$ for the union of the set of poles on the imaginary axis. Assume that $\mathbf{G}(s)$ has constant rank. Then, the interconnected system $\mathbf{G}\#\mathbf{H}$ is stable if*

$$\max_n \bar{\phi}(\mathbf{T}_n(s)) - \min_n \underline{\phi}(\mathbf{T}_n(s)) < \pi, \quad (16)$$

for all $s \in j[0, \infty]$, and

$$\max_e \bar{\phi}(\mathcal{T}_e(s)) - \min_e \underline{\phi}(\mathcal{T}_e(s)) \leq \pi, \quad (17)$$

for all $s \notin j\Omega$, and

$$\sup_{n, e, s \notin j\Omega} [\bar{\phi}(\mathbf{T}_n(s)) + \bar{\phi}(\mathcal{T}_e(s))] < \pi, \quad (18)$$

$$\inf_{n, e, s \notin j\Omega} [\underline{\phi}(\mathbf{T}_n(s)) + \underline{\phi}(\mathcal{T}_e(s))] > -\pi. \quad (19)$$

Remark: \mathbf{H} is stable, and its sectoriality is ensured by (16). \mathbf{G} is semi-stable, and its semi-sectoriality is ensured by (17) and the rank condition. Equations (18)-(19) imply the stability condition of Theorem 2.

Proof. We provide the proof in Appendix A. \square

V. LINEAR FORM OF POWER GRIDS WITH V - q DROOP

To make use of Proposition 3 we have to linearize the power grid model under investigation into an appropriate form. In this section, we show that the power grid can be represented as an interconnected feedback system of two transfer operators: $\mathbf{T}^{\text{nod}}\#\mathcal{T}^{\text{net}}$. \mathbf{T}^{mod} includes all nodal transfer operators from \hat{q}_n and p_n to ρ_n

and ω_n , as in (2). \mathcal{T}^{net} represents the network structure and the physics of the coupling, as it takes ρ and ω as inputs and provides \hat{q} and p as outputs. The fundamental assumption we make is that the nodes can be modeled as voltage sources that react to conditions in the grid. This assumption is most natural in the context of grid-forming actors, such as power plants or grid-forming inverters.

A. Complex frequency notation

As noted above, every node has a complex voltage (representing a balanced three-phase voltage):

$$v_n(t) = V_n(t)e^{j\varphi_n(t)} = e^{\theta(t)_n} = v_d(t) + jv_q(t), \quad (20)$$

and a complex current i_n . The latter is given in terms of the former through the admittance Laplacian \mathbf{Y} :

$$\mathbf{i}(t) = \mathbf{Y} \cdot \mathbf{v}(t) = -j\mathbf{L} \cdot \mathbf{v}(t). \quad (21)$$

As we assume a lossless grid, the matrix $\mathbf{L} = j\mathbf{Y} \in \mathbb{R}^{N \times N}$ is a real, symmetric, positive definite Laplacian. We assume a power invariant transformation from ABC coordinates, so that the apparent power is given by $S_n(t) = v_n(t)\bar{i}_n(t) = p_n(t) + jq_n(t)$ with active power $p_n(t)$ and reactive power $q_n(t)$.

Milano [11] suggests writing the nodal dynamics through the time derivative of the complex phase θ_n , the complex frequency η :

$$\eta_n(t) = \dot{\theta}_n(t), \quad (22)$$

$$\dot{v}_n(t) = \eta_n(t)v_n(t) \quad (23)$$

$$= (\varrho_n(t) + j\omega_n(t))v_n(t). \quad (24)$$

We will drop the explicit time dependence (t) from now on. By considering both, the complex equation and the complex conjugate equation,

$$\dot{v}_n = \eta_n v_n, \quad (25)$$

$$\dot{\bar{v}}_n = \bar{\eta}_n \bar{v}_n, \quad (26)$$

we can switch back and forth between complex and real picture, using a linear transformation. The velocities ϱ_n , ω_n , η_n and $\bar{\eta}_n$ are related by:

$$\begin{bmatrix} \eta_n \\ \bar{\eta}_n \end{bmatrix} = \begin{bmatrix} 1 & j \\ 1 & -j \end{bmatrix} \begin{bmatrix} \varrho_n \\ \omega_n \end{bmatrix} = \mathbf{U} \begin{bmatrix} \varrho_n \\ \omega_n \end{bmatrix}, \quad (27)$$

$$\begin{bmatrix} \varrho_n \\ \omega_n \end{bmatrix} = \frac{1}{2} \begin{bmatrix} 1 & 1 \\ -j & j \end{bmatrix} \begin{bmatrix} \eta_n \\ \bar{\eta}_n \end{bmatrix} = \frac{1}{2} \mathbf{U}^\dagger \begin{bmatrix} \eta_n \\ \bar{\eta}_n \end{bmatrix}, \quad (28)$$

Note that $\mathbf{U}^{-1} = \frac{1}{2}\mathbf{U}^\dagger$, thus $\mathbf{U}/\sqrt{2}$ is a unitary matrix. This means that under \mathbf{U} as coordinate transformation, all pertinent properties of linear dynamical systems are retained.

B. A system of grid-forming actors

We are interested in conditions that guarantee small-signal stability of a heterogeneous system of grid-forming actors, without strong assumptions on their internal structure. As noted above, we assume that we can model the nodes as voltages reacting to the grid state. We assume that the voltages react in a smooth, differentiable manner, and that $V_n > 0$. Thus, ω_n and ϱ_n are defined, and can be chosen as the nodal output variable. Using p_n and q_n as the input that the nodal actor sees from the grid, we can write the general form of a node's behavior in terms of three functions r_n , o_n and \mathbf{f}_n^x :

$$\varrho_n = r_n(\varphi_n, V_n, p_n, q_n, \mathbf{x}_n), \quad (29)$$

$$\omega_n = o_n(\varphi_n, V_n, p_n, q_n, \mathbf{x}_n), \quad (30)$$

$$\dot{\mathbf{x}}_n = \mathbf{f}_n^x(\varphi_n, V_n, p_n, q_n, \mathbf{x}_n). \quad (31)$$

Here, $\mathbf{x}_n \in \mathbb{R}^{n_{\text{var}}}$ are internal states of dimension n_{var} that reflect the inner workings of the grid actor, and are not visible directly in the output v . Examples include generator frequencies, inner-loop DC voltages, or the d - and q -components of internal AC quantities.

We make two assumptions on the form of the functions r_n , o_n and \mathbf{f}_n^x : I) Following [12], we assume that the nodal dynamics does not explicitly depend on φ_n . This assumption is usually true, and is justified by symmetry considerations and the desire to not introduce harmonic disturbances into the grid. II) We assume that the reaction to a deviation in the voltage mirrors that of a deviation in the reactive power. That is, we assume that near the operation point, r_n , o_n and \mathbf{f}_n^x only depend on $\hat{q}_n = q_n + \alpha_n V_n$ for some real α_n rather than on both q_n and V_n separately. With these assumptions we have:

$$\varrho_n = r_n(p_n, \hat{q}_n, \mathbf{x}_n), \quad (32)$$

$$\omega_n = o_n(p_n, \hat{q}_n, \mathbf{x}_n), \quad (33)$$

$$\dot{\mathbf{x}}_n = \mathbf{f}_n^x(p_n, \hat{q}_n, \mathbf{x}_n). \quad (34)$$

C. The linearized nodal response

We define the coefficients of the Jacobian as

$$\begin{aligned} J_n^{\omega p} &:= \frac{\partial o_n}{\partial p_n}, & J_n^{\varrho \hat{q}} &= \frac{\partial r_n}{\partial (\hat{q}_n)}, \\ J_n^{xx} &= \frac{\partial \mathbf{f}_n^x}{\partial \mathbf{x}_n}, & \text{etc.} & \end{aligned} \quad (35)$$

We now want to look at the linear response of the nodal subsystem around an operating point v_n° , i_n° . We assume that the operating point satisfies $\varrho_n^\circ = \omega_n^\circ = \dot{\mathbf{x}}_n^\circ = 0$. Write $\Delta p_n = p_n - p_n^\circ$ and $\Delta \hat{q}_n = q_n - q_n^\circ + \alpha_n (V_n - V_n^\circ)$ and assume that $\mathbf{x}_n^\circ = \mathbf{0}$. The linearized nodal dynamics are then

$$\dot{\mathbf{x}}_n = \mathbf{J}_n^{xp} \Delta p_n + \mathbf{J}_n^{x\hat{q}} \Delta \hat{q}_n + \mathbf{J}_n^{xx} \mathbf{x}_n, \quad (36)$$

$$\varrho_n = J_n^{\varrho p} \Delta p_n + J_n^{\varrho \hat{q}} \Delta \hat{q}_n + J_n^{\varrho x} \mathbf{x}_n, \quad (37)$$

$$\omega_n = J_n^{\omega p} \Delta p_n + J_n^{\omega \hat{q}} \Delta \hat{q}_n + J_n^{\omega x} \mathbf{x}_n. \quad (38)$$

which we stack as

$$\dot{\mathbf{x}}_n = \mathbf{J}_n^{xqp} \begin{bmatrix} \Delta \hat{q}_n \\ \Delta p_n \end{bmatrix} + \mathbf{J}_n^{xx} \mathbf{x}_n, \quad (39)$$

$$\begin{bmatrix} \varrho_n \\ \omega_n \end{bmatrix} = \mathbf{J}_n^{\varrho\omega qp} \begin{bmatrix} \Delta \hat{q}_n \\ \Delta p_n \end{bmatrix} + \mathbf{J}_n^{\varrho\omega x} \mathbf{x}_n. \quad (40)$$

The nodal transfer operator from $[\Delta \hat{q}_n \ \Delta p_n]^\top$ to $[\varrho_n \ \omega_n]^\top$ is then just

$$-\mathbf{T}_n(s) = \mathbf{J}_n^{\varrho\omega \hat{q}p} + \mathbf{J}_n^{\varrho\omega x} (s - \mathbf{J}_n^{xx})^{-1} \mathbf{J}_n^{xqp}. \quad (41)$$

We can summarize the transfer operators of all nodes in \mathbf{T}^{nod} such that

$$\begin{bmatrix} \varrho \\ \omega \end{bmatrix} = \mathbf{T}^{\text{nod}} \begin{bmatrix} \Delta \hat{q} \\ \Delta p \end{bmatrix} := \bigoplus_n \mathbf{T}_n(s) \begin{bmatrix} \Delta \hat{q} \\ \Delta p \end{bmatrix}. \quad (42)$$

D. The linearized network response

To obtain the full linearized equations, we need the response of Δp_n and $\Delta \hat{q}_n$ to variations in the complex angle θ_n around a given power flow with θ_n° .

This is most easily given in terms of a variant of the complex power and the complex couplings introduced by [13]. We define

$$\sigma_n := q_n + jp_n, \quad (43)$$

to mirror the definition of the complex frequency [11]. In terms of the usual complex power, this is $\sigma_n = j\bar{S}_n$. This complex power can be expressed in terms of the Hermitian matrix $\mathbf{K} \in \mathbb{C}^{N \times N}$ of complex couplings [11], [13]:

$$K_{nm} = \bar{v}_n L_{nm} v_m, \quad (44)$$

$$\sigma_n = \sum_m K_{nm}. \quad (45)$$

These quantities have a very simple derivative with respect to the complex phases of the system:

$$\frac{\partial K_{nm}}{\partial \theta_h} = \delta_{hm} K_{nm}, \quad \frac{\partial K_{nm}}{\partial \bar{\theta}_h} = \delta_{hn} K_{nm}, \quad (46)$$

$$\frac{\partial \sigma_n}{\partial \theta_h} = K_{nh}, \quad \frac{\partial \sigma_n}{\partial \bar{\theta}_h} = \delta_{nh} \sigma_n. \quad (47)$$

The linearization of σ_n around an operating state of the system with complex couplings K_{nm}° and complex power σ_n° is then given by

$$\sigma_n \approx \sigma_n^\circ + \sigma_n^\circ \Delta \bar{\theta}_n + \sum_m K_{nm}^\circ \Delta \theta_m, \quad (48)$$

or, in vector notation,

$$\begin{bmatrix} \Delta \sigma \\ \Delta \bar{\sigma} \end{bmatrix} \approx \begin{bmatrix} \mathbf{K}^\circ \\ [\bar{\sigma}^\circ] \end{bmatrix} \begin{bmatrix} \sigma^\circ \\ \bar{\mathbf{K}}^\circ \end{bmatrix} \begin{bmatrix} \Delta \theta \\ \Delta \bar{\theta} \end{bmatrix}. \quad (49)$$

As the nodal dynamics depend on $\Delta \hat{q}_n$ and Δp_n , as inputs, we now consider

$$\Delta \sigma_n + \alpha_n \Delta V_n = \Delta \hat{q}_n + j \Delta p_n, \quad (50)$$

for the output of the edge dynamics. Together with $\Delta V_n \approx V_n^\circ \frac{1}{2} (\Delta \theta + \Delta \bar{\theta})$, we obtain

$$\begin{bmatrix} \Delta \sigma + \alpha \Delta V \\ \Delta \bar{\sigma} + \alpha \Delta V \end{bmatrix} \approx \mathbf{J}^{\text{net}} \begin{bmatrix} \Delta \theta \\ \Delta \bar{\theta} \end{bmatrix}, \quad (51)$$

with the transfer operator

$$\mathbf{J}^{\text{net}} := \begin{bmatrix} \mathbf{K}^\circ + \frac{1}{2} [\alpha] [\mathbf{V}^\circ] & [\sigma^\circ] + \frac{1}{2} [\alpha] [\mathbf{V}^\circ] \\ [\bar{\sigma}^\circ] + \frac{1}{2} [\alpha] [\mathbf{V}^\circ] & \bar{\mathbf{K}}^\circ + \frac{1}{2} [\alpha] [\mathbf{V}^\circ] \end{bmatrix}. \quad (52)$$

Note that as \mathbf{K}° is Hermitian, and so is \mathbf{J}^{net} . Further, we see from (45) that $[\mathbf{1} \ -\mathbf{1}]^\top$ is a zero mode of the network response \mathbf{J}^{net} .

At this point, we can see the necessity of incorporating the V - q droop into the network response. Without the presence of the α_n , \mathbf{J}^{net} would be indefinite and thus not amenable to sectorial analysis.

E. The full system

Above we derived the nodal transfer operator from p_n , $q_n + \alpha_n V_n$ to ϱ_n and ω_n , and the network response from θ_n and $\bar{\theta}_n$ to $\sigma_n + \alpha_n V_n$ and $\bar{\sigma}_n + \alpha_n V_n$. We can now combine these into the full system equations. Recall that

$$\Delta \dot{\theta}_n = \eta_n, \quad (53)$$

$$s \Delta \theta_n = \eta_n, \quad (54)$$

where the latter equation is in Laplace space. Let us introduce $\tilde{\mathbf{U}} \in \mathbb{C}^{2N \times 2N}$,

$$\tilde{\mathbf{U}} = \bigoplus_n \mathbf{U}, \quad (55)$$

With this we can write the network response from a deviation in ϱ and ω to a deviation in \hat{q} and p as

$$\mathcal{T}^{\text{net}}(s) = \frac{1}{2} \tilde{\mathbf{U}}^\dagger \frac{1}{s} \mathbf{J}^{\text{net}} \tilde{\mathbf{U}}. \quad (56)$$

The major remaining challenge to applying Proposition 3 and getting decentralized conditions, is to decompose this operator into edge-wise contributions. As we will see in the next

section, we can treat the network response as a superposition of two-node systems.

The full system $\mathcal{T}^{\text{nod}} \# \mathcal{T}^{\text{net}}$ then has the structure

$$\bigoplus_n \mathcal{T}_n(s) \# \mathcal{T}^{\text{net}}(s). \quad (57)$$

VI. PROOF OF THE MAIN THEOREM 1

We now proceed to the proof of the main theorem. The first step is to provide conditions for the sectoriality of the nodal transfer operators. Then we provide the edge-wise decomposition of the network response, and demonstrate under which conditions it is semi-stable frequency-wise semi-sectorial. The main Theorem then follows by applying Proposition 3.

A. Sectoriality of the nodal transfer operator

Each $\mathcal{T}_n(s)$ of the form (2) is a complex 2×2 matrix. Here, we give conditions that ensure that it is strictly accretive, meaning the numerical range is contained in the open right half plane: $\phi > -\pi/2$ and $\bar{\phi} < \pi/2$. It gives especially concise conditions for sectoriality.

Lemma 4. *A complex 2×2 matrix $\mathcal{T}_n(s)$ is strictly accretive, hence sectorial, if and only if its four entries [see (2)] fulfill (3) and (4):*

$$\Re(\mathcal{T}_n^{\omega p}) + \Re(\mathcal{T}_n^{\varrho \hat{q}}) > 0, \quad (58)$$

$$\Re(\mathcal{T}_n^{\omega p}) \cdot \Re(\mathcal{T}_n^{\varrho \hat{q}}) > \frac{1}{4} \left| \mathcal{T}_n^{\omega \hat{q}} + \bar{\mathcal{T}}_n^{\varrho p} \right|^2. \quad (59)$$

Proof. If the numerical range of \mathcal{T}_n is contained in the right-hand side, the real part of the numerical range has to be strictly positive: $\Re(W(\mathcal{T}_n(s))) > 0$. The real part of the numerical range is given by the numerical range of the Hermitian part of $\mathcal{T}_n(s)$, which we denote $\hat{\mathcal{T}}_n(s) = \frac{1}{2}(\mathcal{T}_n(s) + \mathcal{T}_n(s)^\dagger)$. The numerical range of a Hermitian matrix is on the real axis. It is strictly positive if and only if the matrix is positive definite. The two by two matrix $\hat{\mathcal{T}}_n(s)$ is positive definite if and only if its determinant and its trace are positive. Expressed in terms of the matrix elements of $\mathcal{T}_n(s)$ these conditions are (3) and (4). \square

B. Edge-wise decomposition and analysis of the network response

We now return to the network response. Our goal is to show that under the condition that [see (5)]

$$\alpha_n \geq \alpha_n^{\text{min}} := 2V_n^\circ |Y_{nn}| \left(\frac{\gamma_{\text{max}}}{\cos \Delta \varphi_{\text{max}}} - 1 \right), \quad (60)$$

we can decompose the network response into frequency wise semi-stable and semi-sectorial edge contributions.

Lemma 5. \mathbf{J}^{net} can be decomposed into edge-wise contributions \mathbf{J}_e such that

$$\mathbf{J}^{\text{net}} = \mathbf{B}_+^\dagger \bigoplus_e \mathbf{J}_e \mathbf{B}_+, \quad (61)$$

if we introduce an edge-wise decomposition α'_{nm} of α_n such that

$$\alpha_n = -2V_n^\circ \sum_{m \neq n} L_{nm} \alpha'_{nm}. \quad (62)$$

Proof. The fundamental strategy is to collect the terms that represent each edge. In each of the four blocks of \mathbf{J}^{net} , the off diagonal matrix elements naturally have an edge associated to them. The diagonal elements of \mathbf{K}° can be written as a sum of edge-wise contributions $K_{nn}^\circ = -|V_n^\circ|^2 \sum_{m \neq n} L_{nm}$. The σ° can be written as $\sigma_n^\circ = \sum_{m \neq n} K_{nm}^\circ - |V_n^\circ|^2 \sum_{m \neq n} L_{nm}$. We then introduce a similar decomposition for $\frac{1}{2}\alpha$ times \mathbf{V}° , writing $\frac{1}{2}\alpha_n V_n^\circ = -|V_n^\circ|^2 \sum_{m \neq n} L_{nm} \alpha'_{nm}$. Now, the contributions to the matrix elements of \mathbf{J}^{net} associated to an edge $e = (n, m)$ all live on the rows and columns associated to n and m . Thus, we can place them in a 4×4 matrix \mathbf{J}^e using the operators \mathbf{P}_e of (9) that pick out exactly those rows and columns.

To collect these edge-wise contributions, we introduce $\beta_{nm} = -|V_n^\circ|^2 L_{nm} (1 + \alpha'_{nm})$ and $C_{nm} = K_{nm}^\circ + \beta_{nm}$. Then we can succinctly write the four by four matrix of elements originating from a single edge as:

$$\mathbf{J}_e = \begin{bmatrix} \beta_{nm} & K_{nm}^\circ & C_{nm} & 0 \\ K_{mn}^\circ & \beta_{mn} & 0 & C_{mn} \\ \bar{C}_{nm} & 0 & \beta_{nm} & \bar{K}_{nm}^\circ \\ 0 & \bar{C}_{mn} & \bar{K}_{mn}^\circ & \beta_{mn} \end{bmatrix}. \quad (63)$$

With this, (61) can be verified by straightforward calculation, collecting all terms associated to each edge. \square

As \mathbf{J}^{net} , and the \mathbf{J}_e , are Hermitian, their numerical range is on the real axis. They are (semi-)sectorial, if and only if they are (semi-)definite. In the phase stability theorems, it is assumed that the transfer operator $G(\epsilon^+)$ has phase center zero. From (56) we see that this implies that \mathbf{J}^{net} and thus \mathbf{J}_e have to be positive semi-definite.

Lemma 6. \mathbf{J}_e is positive semi-definite, hence semi-sectorial, if

$$|\varphi_n^\circ - \varphi_m^\circ| < \frac{\pi}{2} \quad \forall e = (n, m) \in \mathcal{E}, \quad (64)$$

$$\alpha'_{nm} \geq \frac{\gamma_{mn}}{\cos(\varphi_n^\circ - \varphi_m^\circ)} - 1. \quad (65)$$

Proof. This can be verified with a straightforward but lengthy calculation using the Schur complement. The detailed calculation is contained in the supplemental material. \square

The edge-wise decomposition of α_n leaves us with the freedom to weight the α'_{nm} freely, as long as they satisfy (62). The tightest bound is achieved by weighting them proportional to the bounds derived in (65). However, we can achieve a much more concise node-wise condition for the α_n , which are actual dynamical parameters of the nodal actors.

Lemma 7. $\mathcal{T}^{\text{net}}(s)$ can be decomposed into semi-stable frequency-wise sectorial \mathcal{T}_e as

$$\mathcal{T}^{\text{net}}(s) = \tilde{\mathbf{U}}^\dagger \mathbf{B}_+^\dagger \bigoplus_e \mathcal{T}_e(s) \mathbf{B}_+ \tilde{\mathbf{U}}, \quad (66)$$

if $\alpha_n \geq \alpha_n^{\min}$, i.e., (5) holds.

Proof. The $\mathcal{T}_e(s)$ are given by

$$\mathcal{T}_e := \frac{1}{2s} \mathbf{J}_e. \quad (67)$$

According to Lemma 6, (64) and (65) imply frequency-wise semi-sectorial \mathbf{J}_e and thus \mathcal{T}_e . The factor $1/s$ makes them semi-stable, because the pole is at zero and the rank left constant along the contour. Using the definition of α'_{nm} we see that (65) can always be satisfied if $\alpha_n \geq \alpha_n^{\min}$. \square

As $\bigoplus_e \mathcal{T}_e(s)$ only depends on s through scaling by a common factor, we also immediately have that its rank is constant along the contour. Thus, $\mathcal{T}^{\text{net}}(s)$ is semi-stable frequency-wise semi-sectorial. On $s \in j(\epsilon^+, \infty]$ the phases of the $\mathcal{T}_e(s)$ are simply:

$$\underline{\phi}(\mathcal{T}_e) = -\frac{\pi}{2}, \quad \bar{\phi}(\mathcal{T}_e) = -\frac{\pi}{2}. \quad (68)$$

on the quarter circle of radius ϵ^+ from $j\epsilon^+$ to ϵ^+ , they rotate to 0.

In conclusion, (5) ensures semi-stable frequency-wise sectorial $\mathcal{T}^{\text{net}}(s)$ with a DC phase center of 0, which is a pole, and all phases $-\frac{\pi}{2}$ at $s \in j(\mathbb{R} \setminus \Omega)$.

C. Putting everything together

Proof. We can now apply Proposition 3 to the system given by (57), with $\mathbf{H} = \mathbf{T}^{\text{mod}} = \bigoplus_n \mathbf{T}_n(s)$, $\mathbf{B} = \mathbf{B}_+ \tilde{\mathbf{U}}$, and $\mathbf{G} = \mathcal{T}^{\text{net}} = \mathbf{B}_+^\dagger \bigoplus_e \mathcal{T}_e(s) \mathbf{B}_+$. Our whole decomposition of the system is illustrated in Fig. 1. We have shown in the previous sections that with (3)-(5), (i) the \mathbf{T}_n in (2) and (41) are in \mathcal{RH}_∞ (hence stable) and frequency-wise sectorial according to Lemma 4; (ii) the \mathcal{T}_e in (67) are semi-stable frequency-wise semi-sectorial according to Lemma 6. \mathbf{G} has constant rank along the contour, because it depends on s only by a prefactor $1/s$.

We now proceed to show that (16)-(19) hold. Equation (16) is fulfilled for (3)-(4), as $\underline{\phi}(\mathbf{T}_n) > -\pi/2$ and $\bar{\phi}(\mathbf{T}_n) < \pi/2$. Equation (17) is fulfilled, as (68) implies zero phase differences

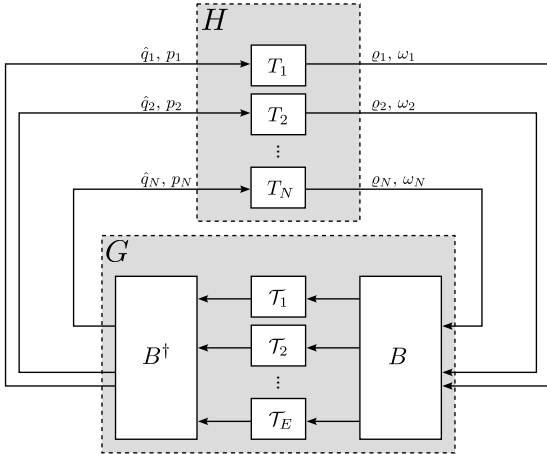


Figure 1: Block diagram representation of the system considered. Block H is the nodal response to the lines' output, and block G is the lines' response to the nodes' dynamics.

for all \mathcal{T}_e and for \mathcal{T}^{net} in total. Similarly, the combined phases of \mathcal{T}^{net} and \mathcal{T}^{mod} lie within $(-\pi, 0)$ at all $s \in j(\mathbb{R} \setminus \Omega)$, hence (18) and (19) hold. This concludes the proof. \square

As \mathcal{T}_e have phase $-\frac{\pi}{2}$ at all non-zero frequencies, the phases of \mathbf{T}_n need not be contained in the open right half plane. However, $\hat{\mathbf{T}}_n > 0$ is sufficient for our examples below and gives the most concise conditions.

VII. EXAMPLES

Here, we demonstrate that a range of systems falls into the class (32)-(34), which can be represented by a transfer operator as in (41) and thus prove stability for those with Theorem 1.

A. Second-order models

Models without internal variables \mathbf{x} have a $-\mathbf{T}_n = \mathbf{J}_n^{e\omega\hat{q}p}$ that is independent of s and therefore real. Equations (3)-(4) become

$$T_n^{e\hat{q}} + T_n^{\omega p} > 0, \quad (69)$$

$$T_n^{e\hat{q}} \cdot T_n^{\omega p} > \frac{1}{4} (T_n^{ep} + T_n^{\omega\hat{q}})^2. \quad (70)$$

The well-established droop principles of controlling φ_n with $-\Delta p_n$ and V_n with $-\Delta q_n$ and $-\Delta V_n$ (see for example [9], [10]) are reflected in $T_n^{\omega p} > 0$ and $T_n^{e\hat{q}} > 0$. Equations (69)-(70) tell us that these coefficients need to have the same sign and need to be positive. Equation (70) further quantifies that cross-coupling, reflected by T_n^{ep} and $T_n^{\omega\hat{q}}$, needs to be sufficiently small in comparison. An example system is the first-

order Kuramoto model with additional voltage control:

$$\tau_{p_n} \dot{\varphi}_n = p_n^\circ - \underbrace{\sum_m (-L_{nm}) V_n V_m \sin(\varphi_n - \varphi_m)}_{p_n}, \quad (71)$$

$$\begin{aligned} \tau_{q_n} \dot{V}_n &= -\alpha_n (V_n - V_n^\circ) \\ &\quad - \sum_m (-L_{nm}) (V_n^2 - V_n V_m \cos(\varphi_n - \varphi_m)) \\ &= -\Delta \hat{q}_n. \end{aligned} \quad (72)$$

The transfer operator is given by

$$-\mathbf{T}_n = \begin{bmatrix} -\tau_{q_n}^{-1} & 0 \\ 0 & -\tau_{p_n}^{-1} \end{bmatrix}. \quad (73)$$

\mathbf{T}_n has phases $\underline{\phi} = \bar{\phi} = 0$ at all s , assuming positive time constants τ_{p_n} and τ_{q_n} .

B. Third-order models

Let us consider models with second-order phase dynamics, and voltage control. For this purpose, we need a single internal variable x_n that represents the phase velocity (angular frequency) relative to the nominal frequency. We further introduce a first-order feed-through term with coefficient δ_n :

$$\dot{\varphi}_n = x_n - \delta_n \Delta p_n, \quad (74)$$

$$\tau_{p_n} \dot{x}_n = -D_n x_n - k_{p_n} \Delta p_n, \quad (75)$$

$$\tau_{q_n} \dot{V}_n = -\Delta V_n - k_{q_n} \Delta q_n. \quad (76)$$

At $\delta_n = 0$ we have pure second-order phase dynamics. We adapted the notation of the droop-controlled inverter model of [4], which we recover at $\delta_n = 0$. With $k_{q_n} = \alpha_n^{-1}$, the transfer operator is given by

$$\mathbf{T}_n = \begin{bmatrix} (V_n^\circ \alpha_n \tau_{q_n})^{-1} & 0 \\ 0 & \delta_n + \frac{k_{p_n}}{s\tau_{p_n} + D_n} \end{bmatrix}, \quad (77)$$

assuming $\tau_{p_n} > 0$ and $\tau_{q_n} > 0$. A similar model is the third-order model for synchronous machines [10] where the voltage dynamics are slightly different:

$$\tau_{V_n} \dot{V}_n = -\Delta V_n - X_n \Delta(q_n/V_n), \quad (78)$$

with transient reactance $X_n \geq 0$. The transfer operators of both models are identical, via the invertible mapping

$$X_n = V_n^\circ k_{q_n} \left(1 + 2 \frac{k_{q_n} q_n^\circ}{V_n^\circ}\right)^{-1}, \quad (79)$$

$$\tau_{V_n} = \tau_{q_n} \left(1 + 2 \frac{k_{q_n} q_n^\circ}{V_n^\circ}\right)^{-1}. \quad (80)$$

This transfer operator also represents the dynamics of virtual synchronous machines [21] and some controls with adaptive inertia [22].

For the nodal transfer matrices to be in \mathcal{RH}_∞ , we need $D_n > 0$. Since the \mathbf{T}_n are diagonal (and thus normal), their numerical range is the line

segment connecting the eigenvalues [18]. Hence, the matrix phases are given by the phases of the diagonal entries. They lie in $(-\frac{\pi}{2}, 0]$ for all $\delta_n > 0$ if $k_{p_n} > -\delta_n D_n$ and $\alpha_n \geq 0$. Only at $\delta_n = 0$, we have $\phi(s = j\infty) = -\frac{\pi}{2}$. In other words, (3)-(4) are fulfilled at all s as long as $\delta_n > 0$.

At $\delta_n = 0$ and $s = j\infty$, we have $T_n^{\omega p} = 0$ and violate (4). The transfer function $\mathbf{T}_n(j\infty)$ is not sectorial, but semi-sectorial at this point. However, this is sufficient to establish semi-stability at $\delta_n = 0$, because stability holds for arbitrarily small δ_n and the eigenvalues of the system's Jacobian are continuous functions of the parameters.

In [4], stability conditions for this model were given in terms of matrix inequalities with a similar interpretation to our analysis: the diagonal couplings $T_n^{\rho \hat{q}}$ and $T_n^{\omega p}$ need to be strong in positive direction, while the off-diagonal cross-coupling need to be bounded relatively. This is quantified in (3)-(4). The more complex structure of \mathbf{T}^{lin} reflects the fact that p and \hat{q} depend on both V and φ , which gives cross-couplings on the network side. It has been reported in [4] that decreasing k_{q_n} can increase stability by weakening the cross-coupling. This is quantified in our lower bound for $\alpha_n = k_{q_n}^{-1}$ in (5):

$$k_{q_n}^{-1} \geq 2V_n^\circ |Y_{nn}| \left(\frac{\gamma_{\max}}{\cos \Delta\varphi_{\max}} - 1 \right), \quad (81)$$

a result that has not yet been reported in the literature. In [23], [24] an upper bound for k_{q_n} was derived that can be tighter or looser depending on the operating points.

As a remark, we can also treat models without voltage amplitude dynamics, like the classical Kuramoto model and the Kuramoto model with inertia, i.e., Swing Equation [1]. To avoid non-sectorial nodal transfer operators due to the lack of voltage dynamics, one has to reduce the representation. One recovers the conditions associated to the frequency dynamics (δ_n, D_n, k_{p_n}) , and gets an additional condition on the ratio between Δp and $\Delta \hat{q}$ in its input. This is expected, as p is known to stabilize phase dynamics, while q results in repulsive coupling in lossless grids [25].

VIII. DISCUSSION AND CONCLUSION

In this paper, we derived fully decentralized small-signal stability conditions for power grids under the assumption of V - q droop and lossless lines. The preceding results provide a simple characterization of small-signal stability of heterogeneous grids in terms of transfer operators between power mismatch on the input side, and frequency and voltage velocity on the output side. Such transfer function-based specifications are natural for the design and specification of

decentralized power grid control strategies, and could potentially be directly encoded in grid codes [26]. This is especially interesting as the transfer functions we are concerned with can be measured experimentally [14].

The type of conditions derived here are robust in the sense that, if the numerical range of a nodal transfer operator is bounded away from zero for all s on the contour, a perturbation of the transfer operator of H_∞ norm smaller than the bound, can not make the system unstable.

Furthermore, this paper aimed for simplicity of results and presentation rather than maximal attainable generality of result. For example, the extension to lossy lines with homogeneous X/R ratio is immediate. On the other hand, allowing fully heterogeneous line parameters is more challenging. Inhomogeneous losses lead to the presence of a non-symmetric zero mode in the line response, which implies non-sectorial behavior. Thus these can not be included easily. A further challenge is to properly account for non-droop-like reactions to the voltage amplitude deviations. Naively adding in additional voltage dynamics on the nodal side fails due to sectoriality constraints. Similarly, models that do not have pass-through do not satisfy the phase condition at $s = j\infty$. Lastly, dVOC [27], [28] is covered by our theorem only in the unloaded case, because $\alpha_n \in \mathbb{R}$. For unloaded grids, (5) states that $\alpha \geq 0$. To deal with these limitations, it will be necessary to properly include gain information in the stability analysis. The companion paper [?] explores this in the context of adaptive network models, we leave this extension of the methods introduced here to future work.

ACKNOWLEDGMENTS

This work was supported by the OpPoDyn Project, Federal Ministry for Economic Affairs and Climate Action (FKZ:03EI1071A).

J.N. gratefully acknowledges support by BIMoS (TU Berlin), Studienstiftung des Deutschen Volkes, and the Berlin Mathematical School, funded by the Deutsche Forschungsgemeinschaft (DFG, German Research Foundation) Germany's Excellence Strategy — The Berlin Mathematics Research Center MATH+ (EXC-2046/1, project ID: 390685689).

R.D. was supported by the Swiss National Science Foundation under grant nr. 200021_215336.

APPENDIX A

PROOF OF PROPOSITION 3

A. Preliminaries

Let us recall two properties of W' that will prove useful later on. First, it follows from the

definition of W' that

$$W'(\mathbf{B}^\dagger \mathbf{M} \mathbf{B}) \subseteq (W'(\mathbf{M}) \cup 0), \quad (82)$$

for any $\mathbf{M} \in \mathbb{C}^{m \times m}$ and \mathbf{B} of appropriate size, and therefore,

$$\overline{\phi}(\mathbf{B}^\dagger \mathbf{M} \mathbf{B}) \leq \overline{\phi}(\mathbf{M}), \quad \underline{\phi}(\mathbf{B}^\dagger \mathbf{M} \mathbf{B}) \geq \underline{\phi}(\mathbf{M}). \quad (83)$$

Second, for a block diagonal system $\mathbf{M} = \bigoplus_e \mathbf{M}_e$, the numerical range is the convex hull of the blocks' numerical ranges [18, Property 1.2.10]:

$$W(\mathbf{M}) = \text{Conv}(W(\mathbf{M}_1), \dots, W(\mathbf{M}_E)). \quad (84)$$

Thus, if \mathbf{M} is semi-sectorial,

$$\overline{\phi}(\mathbf{M}) = \max_e \overline{\phi}(\mathbf{M}_e), \quad \underline{\phi}(\mathbf{M}) = \min_e \underline{\phi}(\mathbf{M}_e). \quad (85)$$

With this toolbox, we are now ready to prove our main result. The proof of Proposition 3 relies on the four following Lemmas.

Lemma 8. *Let $\mathbf{T}_1, \dots, \mathbf{T}_N$ be stable transfer functions. Then $\mathbf{T}(s) = \bigoplus_n \mathbf{T}_n(s)$ is stable.*

Proof. The transfer function $\mathbf{T}(s)$ is stable, because the set of its poles is the union of the poles of its blocks. \square

Lemma 9. *Let $\mathbf{T}_1, \dots, \mathbf{T}_N$ be frequency-wise sectorial transfer functions. Then, $\mathbf{T}(s) = \bigoplus_n \mathbf{T}_n(s)$ is frequency-wise sectorial if and only if*

$$\max_n \overline{\phi}(\mathbf{T}_n(s)) - \min_n \underline{\phi}(\mathbf{T}_n(s)) < \pi, \quad (86)$$

for all $s \in j[0, \infty]$, cf. (16).

Proof. Due to (84), we have that $W(\mathbf{T})$ is the convex hull of all $W(\mathbf{T}_n)$. Therefore, if (86) is satisfied for all, $W(\mathbf{T})$ is contained in a sector of angle $\delta(\mathbf{T}) < \pi$. Furthermore, as none of the $W(\mathbf{T}_n)$ contain the origin, $W(\mathbf{T})$ does not contain the origin. We conclude that \mathbf{T} is frequency-wise sectorial. Similarly, if \mathbf{T} is frequency-wise sectorial, then none of the $W(\mathbf{T}_n)$ contains the origin, and they all lie in a sector of angle smaller than π and (86) holds. All of the above holds for any $s \in j[0, \infty]$, which concludes the proof. \square

Lemma 10. *Let $\mathcal{T}_1, \dots, \mathcal{T}_E$ be semi-stable transfer functions and let us define $\mathcal{T}(s) = \bigoplus_e \mathcal{T}_e(s)$. Let \mathbf{B} be a complex matrix of appropriate dimensions. Then both $\mathcal{T}(s)$ and $\mathbf{B}^\dagger \mathcal{T}(s) \mathbf{B}$ are semi-stable.*

Proof. The transfer function $\mathcal{T}(s)$ is semi-stable, because the set of its poles is the union of the poles of its blocks. As the matrix \mathbf{B} cannot introduce new poles, the poles of $\mathbf{B}^\dagger \mathcal{T}(s) \mathbf{B}$ form a subset of the poles of $\mathcal{T}(s)$. Therefore, $\mathbf{B}^\dagger \mathcal{T}(s) \mathbf{B}$ is semi-stable. \square

Lemma 11. *Let $\mathcal{T}_1, \dots, \mathcal{T}_E$ be frequency-wise semi-sectorial transfer functions and let us define $\mathbf{T}(s) = \bigoplus_e \mathcal{T}_e(s)$. Assume further that*

$$\max_e \overline{\phi}(\mathcal{T}_e(s)) - \min_e \underline{\phi}(\mathcal{T}_e(s)) \leq \pi, \quad (87)$$

for all $s \in j\mathbb{R} \setminus j\Omega$, where $j\Omega$ is the union of the poles of $\mathcal{T}_1, \dots, \mathcal{T}_E$ that lie on the imaginary axis, cf. (17). Assume that $\mathcal{T}_1, \dots, \mathcal{T}_E$ are all frequency-wise semi-sectorial, and assume furthermore that they are semi-sectorial along the indented imaginary axis avoiding the poles of all $\mathcal{T}_e(s)$ for indents smaller than some finite ϵ^* . Finally, assume that $\mathbf{B}^\dagger \mathbf{T}(s) \mathbf{B}$ has constant rank along this indented imaginary axis for some complex matrix \mathbf{B} of appropriate dimensions. Then $\mathbf{B}^\dagger \mathcal{T}(s) \mathbf{B}$ is frequency-wise semi-sectorial.

Remark: $\mathcal{T}(s)$ is covered with $\mathbf{B} = \mathbf{I}$.

Proof. First observe that if a meromorphic $\mathcal{T}_e(s)$ has constant rank r on a contour, it has constant rank on any infinitesimal deformation of the contour. A matrix of rank r has a minor of order r with non-zero determinant, and the determinants of all minors of order larger than r are zero. As the minors are meromorphic functions, they are either identically zero, or their zeros are isolated points. Thus the rank can only change at isolated points of the meromorphic function. As the rank is constant on the contour, none of these points can be on the contour and we can deform the contour avoiding these points.

Take an $\epsilon < \epsilon^*$ such that for all $\epsilon' \leq \epsilon$, the imaginary axis with ϵ' indentation at $j\Omega$ does not hit a rank changing point of any $\mathcal{T}_e(s)$, $e \in \{1, \dots, E\}$.

By assumption, for all $e \in \{1, \dots, E\}$, $\mathcal{T}_e(s)$ is semi-sectorial and has constant rank on this ϵ -indented imaginary axis (contour).

Combining (82), (84), and (87), semi-sectoriality of $\mathcal{T}_1(s), \dots, \mathcal{T}_E(s)$ implies semi-sectoriality of $\mathbf{B}^\dagger \mathcal{T}(s) \mathbf{B}$, for $s \in j\mathbb{R}$.

Furthermore, by assumption, $\mathbf{B}^\dagger \mathcal{T}(s) \mathbf{B}$ has constant rank along the ϵ -indented imaginary axis.

Altogether, the above implies that $\mathbf{B}^\dagger \mathcal{T}(s) \mathbf{B}$ is frequency-wise semi-sectorial, which concludes the proof. \square

B. Proof of Proposition 3

Proof. By Lemma 8, $\mathbf{H} = \bigoplus_n \mathbf{T}_n$ is stable. By Lemma 9, \mathbf{H} is frequency-wise sectorial if (16) holds. By Lemma 10, $\mathbf{G} = \mathbf{B}^\dagger \bigoplus_e \mathcal{T}_e \mathbf{B}$ is semi-stable. By Lemma 11, \mathbf{G} is frequency-wise semi-sectorial, if (17) holds.

Using one more time the convex hull property (84), in particular (85), and the subset property (82), the assumptions (18)-(19) yield

$$\sup_{s \notin j\Omega} \left[\overline{\phi} \left(\bigoplus_n \mathbf{T}_n \right) + \overline{\phi} \left(\mathbf{B}^\dagger \bigoplus_e \mathcal{T}_e \mathbf{B} \right) \right] < \pi, \quad (88)$$

$$\inf_{s \notin j\Omega} \left[\underline{\phi} \left(\bigoplus_n \mathbf{T}_n \right) + \underline{\phi} \left(\mathbf{B}^\dagger \bigoplus_e \mathcal{T}_e \mathbf{B} \right) \right] > -\pi, \quad (89)$$

where \mathbf{T}_n and \mathcal{T}_e are functions of s . These are the phase conditions (14)-(15) of Theorem 2. All in all, the system $(\bigoplus_n \mathbf{T}_n) \# (\mathbf{B}^\dagger \bigoplus_e \mathcal{T}_e \mathbf{B})$ then satisfies all assumptions and conditions of Theorem 2 and is therefore stable, which concludes the proof. \square

REFERENCES

- [1] A. Bergen and D. Hill, "A Structure Preserving Model for Power System Stability Analysis," *IEEE Transactions on Power Apparatus and Systems*, vol. PAS-100, no. 1, pp. 25–35, Jan. 1981. [Online]. Available: <http://ieeexplore.ieee.org/document/4110445/>
- [2] J. Machowski, J. Bialek, and J. Bumby, "Power System Dynamics. Stability and Control," Jan. 2012.
- [3] F. Dörfler, M. Chertkov, and F. Bullo, "Synchronization in complex oscillator networks and smart grids," *Proceedings of the National Academy of Sciences*, vol. 110, no. 6, pp. 2005–2010, Feb. 2013, publisher: Proceedings of the National Academy of Sciences. [Online]. Available: <https://www.pnas.org/doi/full/10.1073/pnas.1212134110>
- [4] J. Schiffer, R. Ortega, A. Astolfi, J. Raisch, and T. Sezi, "Conditions for stability of droop-controlled inverter-based microgrids," *Automatica*, vol. 50, no. 10, pp. 2457–2469, Oct. 2014. [Online]. Available: <https://www.sciencedirect.com/science/article/pii/S0005109814003100>
- [5] D. Witthaut, F. Hellmann, J. Kurths, S. Kettemann, H. Meyer-Ortmanns, and M. Timme, "Collective nonlinear dynamics and self-organization in decentralized power grids," *Reviews of Modern Physics*, vol. 94, no. 1, p. 015005, Feb. 2022, publisher: American Physical Society. [Online]. Available: <https://link.aps.org/doi/10.1103/RevModPhys.94.015005>
- [6] P. Christensen, G. K. Andersen, M. Seidel, S. Bolik, S. Engelken, T. Knueppel, A. Kroniris, K. Wuerflinger, T. Bülo, J. Jahn, and others, "High penetration of power electronic interfaced power sources and the potential contribution of grid forming converters," ENTSO-E, Tech. Rep., 2020. [Online]. Available: https://eepublicdownloads.entsoe.eu/clean-documents/Publications/SOC/High_Penetration_of_Power_Electronic_Interfaced_Power_Sources_and_the_Potential_Contribution_of_Grid_Forming_Converters.pdf
- [7] A. Dyško, A. Egea, Q. Hong, A. Khan, P. Ernst, R. Singer, and Ise, "Testing Characteristics of Grid Forming Converters Part III: Inertial Behaviour"
- [8] X. He, L. Huang, I. Subotić, V. Häberle, and F. Dörfler, "Quantitative Stability Conditions for Grid-Forming Converters With Complex Droop Control," *IEEE Transactions on Power Electronics*, vol. 39, no. 9, pp. 10834–10852, Sep. 2024. [Online]. Available: <https://ieeexplore.ieee.org/document/10536651/>
- [9] J. Schiffer, D. Zonetti, R. Ortega, A. M. Stanković, T. Sezi, and J. Raisch, "A survey on modeling of microgrids—From fundamental physics to phasors and voltage sources," *Automatica*, vol. 74, pp. 135–150, Dec. 2016. [Online]. Available: <https://www.sciencedirect.com/science/article/pii/S0005109816303041>
- [10] K. Schmietendorf, J. Peinke, R. Friedrich, and O. Kamps, "Self-organized synchronization and voltage stability in networks of synchronous machines," *The European Physical Journal Special Topics*, vol. 223, no. 12, pp. 2577–2592, Oct. 2014. [Online]. Available: <https://doi.org/10.1140/epjst/e2014-02209-8>
- [11] F. Milano, "Complex Frequency," *IEEE Transactions on Power Systems*, vol. 37, no. 2, pp. 1230–1240, Mar. 2022, conference Name: IEEE Transactions on Power Systems. [Online]. Available: https://ieeexplore.ieee.org/abstract/document/9524491?casa_token=d7Q69Fh7p2sAAAAA:ZxtL-BmdodQ47xJMfr2Gk3wyoqBFbQCOFjm8uW_sHv6mvdmg52mYhzps7b5w6tGxi7mz1Ytqygt
- [12] R. Kogler, A. Plietzsch, P. Schultz, and F. Hellmann, "Normal Form for Grid-Forming Power Grid Actors," *PRX Energy*, vol. 1, no. 1, p. 013008, Jun. 2022, publisher: American Physical Society. [Online]. Available: <https://link.aps.org/doi/10.1103/PRXEnergy.1.013008>
- [13] A. Büttner and F. Hellmann, "Complex Couplings - A Universal, Adaptive, and Bilinear Formulation of Power Grid Dynamics," *PRX Energy*, vol. 3, no. 1, p. 013005, Feb. 2024, publisher: American Physical Society. [Online]. Available: <https://link.aps.org/doi/10.1103/PRXEnergy.3.013005>
- [14] A. Büttner, H. Würfel, S. Liemann, J. Schiffer, and F. Hellmann, "Complex-Phase, Data-Driven Identification of Grid-Forming Inverter Dynamics," Sep. 2024, arXiv:2409.17132. [Online]. Available: <http://arxiv.org/abs/2409.17132>
- [15] L. Huang, D. Wang, X. Wang, H. Xin, P. Ju, K. H. Johansson, and F. Dörfler, "Gain and Phase: Decentralized Stability Conditions for Power Electronics-Dominated Power Systems," Sep. 2023, arXiv:2309.08037 [cs, eess]. [Online]. Available: <http://arxiv.org/abs/2309.08037>
- [16] L. Woolcock and R. Schmid, "Mixed Gain/Phase Robustness Criterion for Structured Perturbations With an Application to Power System Stability," *IEEE Control Systems Letters*, vol. 7, pp. 3193–3198, 2023, conference Name: IEEE Control Systems Letters. [Online]. Available: <https://ieeexplore.ieee.org/document/10167642/authors#authors>
- [17] W. Chen, D. Wang, S. Z. Khong, and L. Qiu, "A Phase Theory of Multi-Input Multi-Output Linear Time-Invariant Systems," *SIAM Journal on Control and Optimization*, vol. 62, no. 2, pp. 1235–1260, Apr. 2024. [Online]. Available: <https://epubs.siam.org/doi/10.1137/22M148968X>
- [18] R. A. Horn and C. R. Johnson, *Topics in Matrix Analysis*, 1st ed. Cambridge University Press, Apr. 1991. [Online]. Available: <https://www.cambridge.org/core/product/identifier/9780511840371/type/book>
- [19] D. Wang, W. Chen, S. Z. Khong, and L. Qiu, "On the phases of a complex matrix," *Linear Algebra and its Applications*, vol. 593, pp. 152–179, May 2020. [Online]. Available: <https://www.sciencedirect.com/science/article/pii/S0024379520300458>
- [20] D. Wang, X. Mao, W. Chen, and L. Qiu, "On the phases of a semi-sectorial matrix and the essential phase of a Laplacian," *Linear Algebra and its Applications*, vol. 676, pp. 441–458, Nov. 2023. [Online]. Available: <https://www.sciencedirect.com/science/article/pii/S0024379523002744>
- [21] Z. Shuai, C. Shen, X. Liu, Z. Li, and Z. J. Shen, "Transient Angle Stability of Virtual Synchronous Generators Using Lyapunov's Direct Method," *IEEE Transactions on Smart Grid*, vol. 10, no. 4, pp. 4648–4661, Jul. 2019, conference Name: IEEE Transactions on Smart Grid. [Online]. Available: <https://ieeexplore.ieee.org/document/8444083?arnumber=8444083>
- [22] J. Fritzsche and P. Jacquod, "Stabilizing Large-Scale Electric Power Grids with Adaptive Inertia," *PRX Energy*, vol. 3, no. 3, p. 033003, Aug.

- 2024, publisher: American Physical Society. [Online]. Available: <https://link.aps.org/doi/10.1103/PRXEnergy.3.033003>
- [23] P. C. Böttcher, D. Witthaut, and L. Rydin Gorjão, “Dynamic stability of electric power grids: Tracking the interplay of the network structure, transmission losses, and voltage dynamics,” *Chaos: An Interdisciplinary Journal of Nonlinear Science*, vol. 32, no. 5, p. 053117, May 2022. [Online]. Available: <https://doi.org/10.1063/5.0082712>
- [24] P. C. Böttcher, L. R. Gorjão, and D. Witthaut, “Stability Bounds of Droop-Controlled Inverters in Power Grid Networks,” *IEEE Access*, vol. 11, pp. 119 947–119 958, 2023, conference Name: IEEE Access. [Online]. Available: <https://ieeexplore.ieee.org/document/10267988/?arnumber=10267988>
- [25] D. Anderson, A. Tenzer, G. Barlev, M. Girvan, T. M. Antonsen, and E. Ott, “Multiscale dynamics in communities of phase oscillators,” *Chaos: An Interdisciplinary Journal of Nonlinear Science*, vol. 22, no. 1, p. 013102, Jan. 2012. [Online]. Available: <https://doi.org/10.1063/1.3672513>
- [26] V. Häberle, L. Huang, X. He, E. Prieto-Araujo, and F. Dörfler, “Dynamic Ancillary Services: From Grid Codes to Transfer Function-Based Converter Control,” Oct. 2023, arXiv:2310.01552 [cs, eess]. [Online]. Available: <http://arxiv.org/abs/2310.01552>
- [27] G.-S. Seo, M. Colombino, I. Subotic, B. Johnson, D. Groß, and F. Dörfler, “Dispatchable Virtual Oscillator Control for Decentralized Inverter-dominated Power Systems: Analysis and Experiments,” in *2019 IEEE Applied Power Electronics Conference and Exposition (APEC)*, Mar. 2019, pp. 561–566, iSSN: 2470-6647. [Online]. Available: <https://ieeexplore.ieee.org/document/8722028>
- [28] D. Groß, M. Colombino, J.-S. Brouillon, and F. Dörfler, “The Effect of Transmission-Line Dynamics on Grid-Forming Dispatchable Virtual Oscillator Control,” *IEEE Transactions on Control of Network Systems*, vol. 6, no. 3, pp. 1148–1160, Sep. 2019, conference Name: IEEE Transactions on Control of Network Systems. [Online]. Available: <https://ieeexplore.ieee.org/abstract/document/8732453>

Supplementary material to: Small-signal stability of power systems with voltage droop

I. CONDITIONS FOR SEMI-SECTORIALITY OF THE EDGE-WISE TRANSFER MATRIX

We want to find conditions under which the four by four matrix

$$\mathbf{J}_e = \begin{pmatrix} \beta_{nm} & K_{nm}^\circ & C_{nm} & 0 \\ K_{mn}^\circ & \beta_{mn} & 0 & C_{mn} \\ \bar{C}_{nm} & 0 & \beta_{nm} & \bar{K}_{nm}^\circ \\ 0 & \bar{C}_{mn} & \bar{K}_{mn}^\circ & \beta_{mn} \end{pmatrix} \quad (1)$$

is positive semi-definite.
Recall that

$$K_{nm}^\circ = v_n^\circ L_{nm} \bar{v}_m^\circ \quad (2)$$

$$\beta_{nm} = -|V_n^\circ|^2 L_{nm} (1 + \alpha'_{nm}) \quad (3)$$

$$C_{nm} = K_{nm}^\circ - |V_n^\circ|^2 L_{nm} (1 + \alpha'_{nm}) . \quad (4)$$

In particular, we have $C_{nm} = K_{nm}^\circ + \beta_{nm}$ and the vector $(1, 1, -1, -1)$ has eigenvalue 0, thus we know $\det \mathbf{J}_e = 0$. To further simplify the equations, we can factor \mathbf{J}_e using the following diagonal matrix:

$$\mathbf{R} = \begin{pmatrix} v_n^\circ & 0 & 0 & 0 \\ 0 & 0 & \bar{v}_n^\circ & 0 \\ 0 & v_m^\circ & 0 & 0 \\ 0 & 0 & 0 & \bar{v}_m^\circ \end{pmatrix} \quad (5)$$

to obtain

$$\mathbf{J}_e = (-L_{nm}) \mathbf{R} \tilde{\mathbf{J}}_e \mathbf{R}^\dagger \quad (6)$$

$$\tilde{\mathbf{J}}_e = \begin{pmatrix} 1 + \alpha'_{nm} & C'_{nm} & -1 & 0 \\ \bar{C}'_{nm} & 1 + \alpha'_{nm} & 0 & -1 \\ -1 & 0 & 1 + \alpha'_{mn} & C'_{mn} \\ 0 & -1 & \bar{C}'_{mn} & 1 + \alpha'_{mn} \end{pmatrix} \quad (7)$$

with

$$-L_{nm} v_n^{\circ 2} C'_{nm} = K_{nm}^\circ + |V_n^\circ|^2 L_{nm} (1 + \alpha'_{nm}) \quad (8)$$

$$C'_{nm} = \frac{\bar{v}_n^\circ}{v_n^\circ} (1 + \alpha'_{nm}) - \frac{\bar{v}_m^\circ}{v_n^\circ} . \quad (9)$$

$$(10)$$

As \mathbf{R} is invertible if $V_n^\circ > 0$, \mathbf{J}_e is positive semi-definite if and only if $\tilde{\mathbf{J}}_e$ is. Introduce the matrix

$$\mathbf{A}_e := \begin{pmatrix} 1 + \alpha'_{nm} & C'_{nm} \\ \bar{C}'_{nm} & 1 + \alpha'_{nm} \end{pmatrix} \quad \text{such that} \quad (11)$$

$$\tilde{\mathbf{J}}_e = \begin{pmatrix} \mathbf{A}_e & -\mathbf{I} \\ -\mathbf{I} & \mathbf{A}_{\bar{e}} \end{pmatrix} \quad (12)$$

with $e = (n, m)$ and $\bar{e} = (m, n)$. \mathbf{A}_e is Hermitian, and it is positive definite if and only if its trace and determinant are. The trace condition is simply:

$$\alpha'_{nm} > -1 . \quad (13)$$

Then, $\det(\mathbf{A}_e) > 0$ if and only if

$$(1 + \alpha'_{nm})^2 - |C'_{nm}|^2 > 0 \quad (14)$$

$$(1 + \alpha'_{nm})^2 - \left(\frac{\bar{v}_n^\circ}{v_n^\circ} (1 + \alpha'_{nm}) - \frac{\bar{v}_m^\circ}{v_m^\circ} \right) \left(\frac{v_n^\circ}{\bar{v}_n^\circ} (1 + \alpha'_{nm}) - \frac{v_m^\circ}{\bar{v}_m^\circ} \right) > 0 \quad (15)$$

$$(1 + \alpha'_{nm}) 2\Re \left(\frac{\bar{v}_n^\circ v_m^\circ}{V_n^{\circ 2}} \right) - \frac{V_m^{\circ 2}}{V_n^{\circ 2}} > 0. \quad (16)$$

This can only be fulfilled for $\Re(\bar{v}_n^\circ v_m^\circ) > 0$, i.e., $V_n^\circ > 0$ for all n and $|\varphi_n^\circ - \varphi_m^\circ| < \pi/2$ for all $e = (n, m) \in \mathcal{E}$. Taking this standard assumption, we get that $\det(\mathbf{A}_e) > 0$ if and only if

$$1 + \alpha'_{nm} > \frac{V_m^{\circ 2}}{2\Re(\bar{v}_n^\circ v_m^\circ)}. \quad (17)$$

Introduce $\gamma_{nm} = V_n^\circ/V_m^\circ = \gamma_{mn}^{-1}$ and $c_{nm} = \cos(\varphi_n^\circ - \varphi_m^\circ) = c_{mn}$. Then, we have $\Re(\bar{v}_m^\circ v_n^\circ) = V_m^\circ V_n^\circ c_{nm}$, and we can write the determinant of \mathbf{A}_e as:

$$\det(\mathbf{A}_e) = (1 + \alpha'_{nm}) 2c_{nm} \gamma_{mn} - \gamma_{mn}^2, \quad (18)$$

and the positivity condition simplifies to

$$1 + \alpha'_{nm} > \frac{\gamma_{mn}}{2c_{nm}}. \quad (19)$$

Now if this condition is satisfied, the Schur complement of \mathbf{A}_e in the transformed $\tilde{\mathbf{J}}_e$ is just:

$$\mathbf{S}_e := \tilde{\mathbf{J}}_e / \mathbf{A}_e := \mathbf{A}_e - (\mathbf{A}_{\bar{e}})^{-1}. \quad (20)$$

Recall that $\det(\tilde{\mathbf{J}}_e) = \det(\mathbf{A}_e) \cdot \det(\mathbf{S}_e)$. As $\tilde{\mathbf{J}}_e$ has a zero mode, but \mathbf{A}_e does not by assumption, the Schur complement \mathbf{S}_e has determinant zero. It is then positive semi-definite if and only if the trace is greater than zero. The trace of the inverse of a two by two matrix satisfies $\text{tr}(\mathbf{A}^{-1}) = \text{tr}(\mathbf{A}) / \det(\mathbf{A})$. Thus, the Schur complement is positive definite if and only if:

$$\text{tr}(\mathbf{A}_e) - \text{tr}(\mathbf{A}_{\bar{e}}) \frac{1}{\det(\mathbf{A}_{\bar{e}})} \geq 0, \quad \text{i.e.,} \quad (21)$$

$$1 + \alpha'_{nm} \geq \frac{1 + \alpha'_{mn}}{\det(\mathbf{A}_{\bar{e}})}. \quad (22)$$

Assume:

$$1 + \alpha'_{nm} > 0 \quad (23)$$

$$1 + \alpha'_{mn} > 0 \quad (24)$$

$$\det(\mathbf{A}_{\bar{e}}) > 0 \quad (25)$$

$$\det(\mathbf{A}_e) > 0, \quad (26)$$

then the Schur complement condition $\text{tr} \mathbf{S}_e \geq 0$ can be recast as follows:

$$1 + \alpha'_{nm} \geq \frac{1 + \alpha'_{mn}}{\det(\mathbf{A}_{\bar{e}})} \quad (27)$$

$$\frac{1 + \alpha'_{mn}}{1 + \alpha'_{nm}} \leq \det(\mathbf{A}_{\bar{e}}) \quad (28)$$

$$\frac{1 + \alpha'_{mn}}{1 + \alpha'_{nm}} \leq (1 + \alpha'_{mn}) 2c_{mn} \gamma_{nm} - \gamma_{nm}^2 \quad (29)$$

$$\frac{1}{1 + \alpha'_{nm}} \leq 2c_{mn} \gamma_{nm} - \gamma_{nm}^2 \frac{1}{1 + \alpha'_{mn}} \quad (30)$$

$$\frac{\gamma_{mn}}{1 + \alpha'_{nm}} \leq 2c_{mn} - \frac{\gamma_{nm}}{1 + \alpha'_{mn}} \quad (31)$$

$$\frac{\gamma_{mn}}{1 + \alpha'_{nm}} + \frac{\gamma_{nm}}{1 + \alpha'_{mn}} \leq 2c_{mn}. \quad (32)$$

This can be satisfied by requiring

$$1 + \alpha'_{nm} \geq \frac{\gamma_{mn}}{c_{nm}} \quad (33)$$

$$1 + \alpha'_{mn} \geq \frac{\gamma_{nm}}{c_{nm}} . \quad (34)$$

These conditions are equivalent via permuting n and m . They also ensure that $\det(\mathbf{A}_{\bar{e}})$ and $\det(\mathbf{A}_e)$ are positive. Altogether, \mathbf{J}_e is positive semi-definite if

$$|\varphi_n^\circ - \varphi_m^\circ| < \frac{\pi}{2} \quad \forall e = (n, m) \in \mathcal{E}, \quad \text{and} \quad (35)$$

$$\alpha'_{nm} \geq \frac{\gamma_{mn}}{\cos(\varphi_n^\circ - \varphi_m^\circ)} - 1 . \quad (36)$$

Aggregated over all edges, we get

$$\alpha_n \geq -2V_n^\circ \sum_{m \neq n} L_{nm} \left(\frac{\gamma_{mn}}{\cos(\varphi_n^\circ - \varphi_m^\circ)} - 1 \right) . \quad (37)$$